

# MANUFACTURE OF ALUMINUM CLOSED-CELL FOAM BY ARB PROCESS USING $\text{CaCO}_3$ AS THE BLOWING AGENT

H. Fathi, E. Emadoddin\* and A. Habibolahzadeh

\* emadoddin@semnan.ac.ir

Received: March 2012

Accepted: June 2012

Department of Materials Engineering, Engineering Faculty, Semnan University, Semnan, Iran.

**Abstract:** The aim of the present study is to fabricate aluminum closed-cell foam via accumulative roll-bonding (ARB) technique using calcium carbonate ( $\text{CaCO}_3$ ) as the blowing agent. Calcium carbonate is an inexpensive material and imparts relatively high porosity to the produced foam. The effects of heating rate, foaming temperature and time on percentage of porosity have been investigated. The results show that increasing the foaming temperature and time results in improvements in the foaming process. It is also shown that the heating rate does not have any effect on the percentage of porosity. Pores have spherical shape and they form in a regular structure by use of  $\text{CaCO}_3$  as the blowing agent. Sample should be heated up abruptly using  $\text{TiH}_2$  as the blowing agent from decomposition temperature of  $\text{TiH}_2$  to foaming temperature in order to gain high porosity foam. It is found that increasing the numbers of accumulative rolling cycle causes uniform distribution of calcium carbonate powder and increases porosity in the final foam by up to 55%.

**Keyword:** Accumulative roll bonding (ARB), Porous material, Aluminum, Foaming, Calcium carbonate blowing agent

## 1. INTRODUCTION

Metal porous foams have been eliciting much interest in recent years due to their high capacity of energy absorption. The characteristics of the pores in these materials play an important role on their energy absorption capability and other properties. Metal foams were first studied in the 1940s; the earliest report is a patent [1]. Materials with porous structures are fascinating in order to combine the physical and mechanical properties and are routinely used for many applications. For example, foamed aluminum is an ultra-light product with closed pores or cell structure. Their high stiffness with low weight makes them useful in automobile applications. The possibility of air penetration and high thermal conductivity makes this material suitable for aerospace and aircraft parts. Other particular properties such as a good energy absorption, high strength and electrical resistance make metal foams useful for applications that require these specific characteristics. Such applications are typically in the construction sector such as automobile manufacturing, light weight civil constructions, noise control in aerospace manufacturing, ship building, railways and sporting equipment [2-6]. Aluminum based metal matrix composites are also appropriate materials for structural

applications in the aircraft and automotive industries because they are lightweight and have a high strength to weight ratio [7]. In the other word, Aluminum based metal matrix composites have some advantages same as metallic foams.

Aluminum foams are typically manufactured by melt and powder metallurgy processes. Melting route is a cheap manufacturing process, and it is possible to control the mechanical properties of the foam by adding necessary alloy elements and additives. Although, the powder metallurgy process offers good control over the cell shape, size, and porosity distribution, it is an expensive method especially to produce complex shapes [8, 9].

In the recent years, much attention has been paid on the process of severe plastic deformation (SPD) which improves mechanical properties of metals and alloys. Large strain deformation processing techniques such as accumulative roll bonding (ARB) and equal channel angular pressing (ECAP) have been developed around the production of ultrafine grained materials [10] and equal channel angular extrusion (ECAE) is a promising technique for production of ultra-fine grain (UFG) materials of few hundred nanometers size [11]. ARB process has been used in modern industries to fabricate layer composites and ultrafine grained structures.

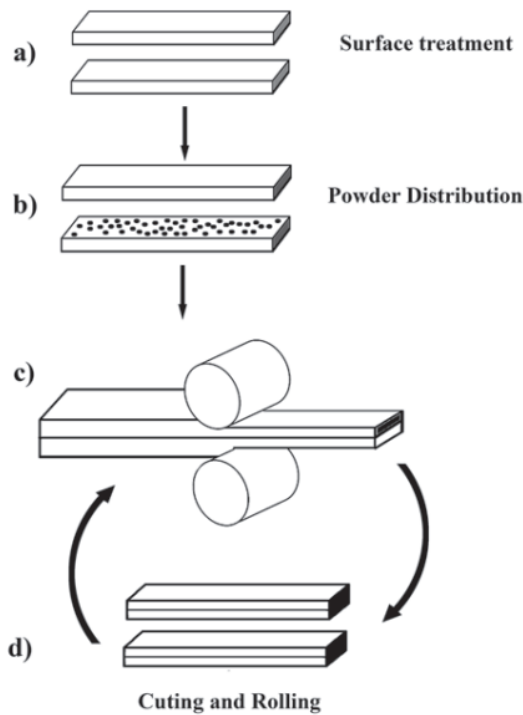


Fig. 1. Applying ARB process for manufacturing of foam, schematically.

Metal forming processes such as ARB can potentially be used for manufacturing of aluminum closed-cell foams. This procedure is schematically illustrated in Fig.1. ARB process possesses the following advantages:

- ARB is a low-cost process and many metallic materials such as aluminum sheets can be processed by this method.
- Rolling of initial sheet stacks is a simple process.

Powder processing, as an essential step in powder metallurgy, would be eliminated in ARB process and then this technique can also be employed for processing of widely industrial alloy [12].

The pore characteristics of the foam play an important role in its physical and mechanical properties. There have been many studies to control the shape, size and distribution of pores to optimize the properties of metallic foams [3, 8]. The manufacturing process parameters and the type of blowing agent used to have a significant

effect on the characteristics of the foams, but these have not been studied in much detail. There are many reports regarding the use of TiH<sub>2</sub> as the foaming agent but there are no studies through the use of CaCO<sub>3</sub>.

This paper reports a novel route to fabricate aluminum closed-cell foam through ARB using CaCO<sub>3</sub> as the blowing agent. CaCO<sub>3</sub> is better than TiH<sub>2</sub> as a foaming additive because it is cheaper, produces spherical pores, requires less heating rate and results in higher porosity. Furthermore, the effect of heating rate, temperature and time during foaming procedure on the porosity is reported for this study.

## 2. EXPERIMENTAL PROCEDURE

### 2. 1. ARB Sample Preparation

A commercial Aluminum 1050 sheet with initial thickness of 5.00 mm was used for this study. It was cold rolled into a 3 mm thick sheet. The aluminum sheet was then cut into 30×150 mm<sup>2</sup> strips and annealed at 350°C for 1h in order to eliminate any strain hardening due to primary cold rolling. The strips were washed with acetone to eliminate any superficial contamination. Both sides of the strips were brushed by a stainless steel wire brush in order to increase the roughness of surfaces to get an excellent bonding between layers. The rolling process was carried out without any lubricant to achieve good friction between surfaces of the mill rolls and the strips.

The blowing agent was CaCO<sub>3</sub> powder with weight percent of 0.5% and size of less than 15µm. This powder was uniformly distributed between two stacked strips. The two strips were then fixed and fastened together with copper wires through four drilled holes near the corners, as shown in Fig. 2. The stack was heated at 200 °C for



Fig. 2. Four corner-drilled holes to fasten aluminum strips together

5 min to provide higher strength bonding [13]. Later, it was rolled to 50% reduction to obtain a mean strain of 0.8. The thickness and length of composite at the end of this process were 3 mm and 300 mm, respectively. According to the energy barrier theory, the threshold deformation increases with the presence of impurities to achieve a good bonding [14]. Therefore, threshold deformation should be increased in order to yield well bounded layers when  $\text{CaCO}_3$  powder is distributed as impurity particles between the strips. The resultant strip was halved and annealed at  $200^\circ\text{C}$  for 10 min to achieve a good bonding after first pass. The halved strips were stacked again over each other without adding any further blowing agent. Second pass of rolling was carried out similar to the first pass. The procedures were repeated up to six passes. The resultant strip, 300 mm long and 3 mm thick, was cut into samples with  $20 \times 10$  mm dimensions for further foaming treatment.

Number of the aluminum layers and  $\text{CaCO}_3$  layers after each cycle can be calculated by equations (1) and (2), respectively.

$$\text{Number of Aluminum layers} = 2^n \quad (1)$$

$$\text{Number of CaCO}_3 \text{ layers} = 2^{n-1} \quad (2)$$

Where  $n$  is number of rolling cycles. Equivalent strain ( $\epsilon_{\text{eq}}$ ) is calculated as follows:

$$\epsilon_{\text{eq}} = \left( \frac{2}{\sqrt{3}} \ln 2 \right) 8 \times n = 0.8n \quad (3)$$

After each cycle, the strip was sectioned and polished to observe bonding interfaces and distribution of  $\text{CaCO}_3$  particles in ARB-ed sheets by scanning electron microscopy.

## 2. 2. Foaming Condition

The final strips were treated in a tubular three-zone furnace to decompose  $\text{CaCO}_3$  under different heating rates and also under various foaming temperatures and times to obtain optimum conditions of foaming. Effect of these parameters on size and distribution of porosity in the samples was studied. The general heat treating profile is shown in Fig. 3. After heating and holding the strips at  $300^\circ\text{C}$  for 600s, they were heated with a

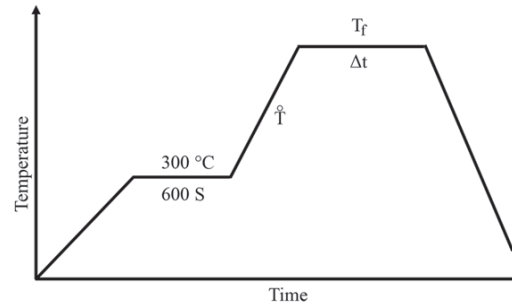


Fig. 3. Heat treating profile used for foaming procedure

heating rate of  $\dot{T} = 5, 10$  and  $20^\circ\text{C/s}$  up to  $T_f = 700^\circ\text{C}$  and holding for a time  $\Delta t = 3$  minutes (Fig. 3). Later they were cooled to room temperature. More experiments were performed at temperature range of  $660\text{--}720^\circ\text{C}$  with holding time of 3-8 minutes.

The porosity of foamed samples was measured by the Archimedes principle and using equation (4):

$$P = \frac{\rho_t - \rho}{\rho_t} \quad (4)$$

Where  $\rho_t$  is the theoretical density,  $\rho$  is the material density [15].

## 3. RESULTS AND DISCUSSION

### 3. 1. Distribution of $\text{CaCO}_3$ Particles via Rolling Cycles

The interfaces between Al-layers are clearly observable due to the existence of the  $\text{CaCO}_3$  particles in primary cycles of ARB up to the third pass (Fig. 4). It is difficult to identify the bonding interfaces beyond the fourth pass of the rolling cycle. This shows that the  $\text{CaCO}_3$  particles were finely and uniformly dispersed throughout the matrix as the rolling cycle increases to six passes. Fig. 4e shows the uniform surface after the 6th rolling cycle without any sharp interface of the  $\text{CaCO}_3$  layer. In this instance, 32 layers of  $\text{CaCO}_3$  (Eq. 2) have been distributed among 64 aluminum layers (Eq. 1) with an approximate thickness of  $47\ \mu\text{m}$ . Calcium carbonate layers are about  $22\ \mu\text{m}$ ,  $12\ \mu\text{m}$  and  $7\ \mu\text{m}$  thick after the first, second and third cycle

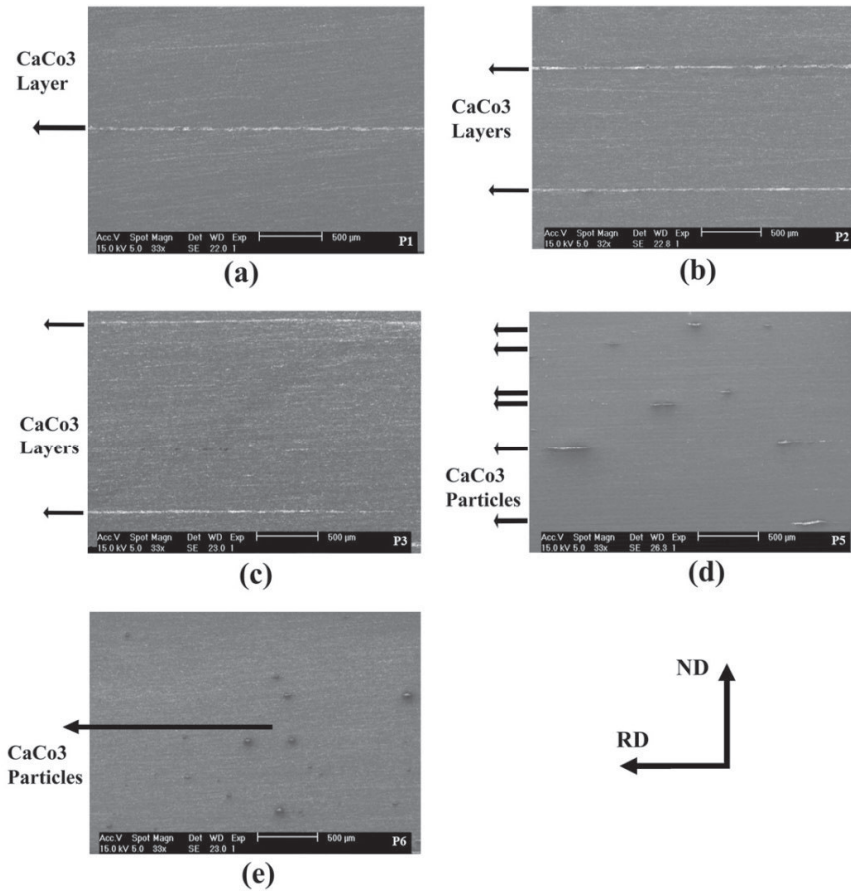


Fig. 4. Bonding interface after (a): first; (b): second; (c): third; (d): fifth; and (e): sixth cycles of ARB

of ARB, respectively, (Fig.4), and they reduce to be almost half thick after each ARB stage. This means that the bonding interfaces are quite fine and  $\text{CaCO}_3$  particles are fairly dispersed throughout the matrix and are not easily detectable (Fig.4e).

Increasing the rolling cycle results in higher strain to the blowing agent and  $\text{CaCO}_3$  particles split further into smaller sizes and uniformly distribute themselves within the matrix. It is suggested [16] that the fine particles lead to increase the gas releasing sites and consequently, the percentage of porosity will be increased.

### 3. 2. Effect of Processing Parameters on Percent of Porosity

Volume of  $\text{H}_2$  and  $\text{CO}_2$  are calculated below in the STP condition. Weight of the strips was 90 g.

Therefore, 0.5wt% of powders would be 0.45 g.

$$T_i \text{H}_2 = T_i + \text{H}_2 \quad (5)$$

$$\frac{50 \text{ g}}{0.45 \text{ g}} = \frac{2 \text{ g}}{A} \Rightarrow A = 0.018 \text{ g}$$

Where, A is the volume of the released hydrogen in gram.

A has to be transferred into the liter in order to compare the volume gas of  $\text{H}_2$  and  $\text{CO}_2$ :

$$\frac{2 \text{ g}}{0.018 \text{ g}} = \frac{22.4 \text{ lit}}{B} \Rightarrow B = 0.2 \text{ lit}$$

Where, B is the volume of the released  $\text{H}_2$  in liter.

Similarly, volume of the  $\text{CO}_2$  could be calculated:

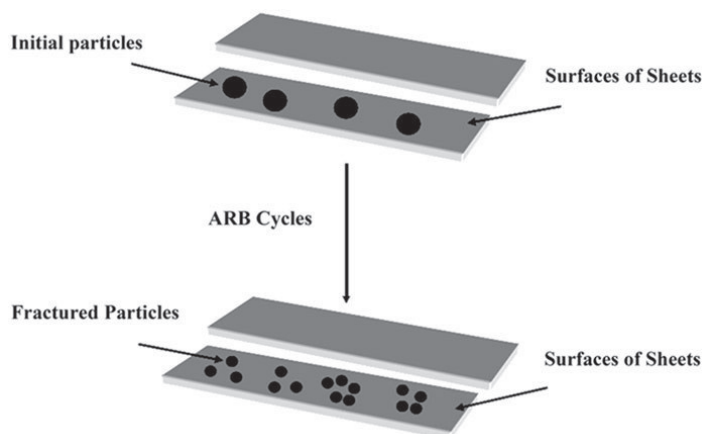


Fig. 5. Effect of ARB cycles on the particles size, schematically.



$$\begin{array}{l} 100 \text{ g} \\ 0.45 \text{ g} \end{array} = \begin{array}{l} 44 \text{ g} \\ D=0.198 \text{ g} \end{array}$$

Where, D is the volume of the released CO<sub>2</sub> in gram.

D has to be transferred into the liter:

$$\begin{array}{l} 44 \text{ g} \\ 0.198 \text{ g} \end{array} = \begin{array}{l} 22.4 \text{ lit} \\ E= 0.1 \text{ lit} \end{array}$$

Where, E is the volume of the released CO<sub>2</sub> in liter.

In the STP condition, the volume of the H<sub>2</sub> and CO<sub>2</sub> are 0.2 and 0.1 lit, respectively. In the other

word, the volume of released gas by CaCO<sub>3</sub> is half the volume of gas released by an equal amount of TiH<sub>2</sub>. It is cleared that the amount of the CaCO<sub>3</sub> has to be increased up to 1wt% to obtain equal volume gas, but it is not practical due to the barrier energy as mentioned in the section 2.1.

The gas released volume by decomposition of 0.5wt% CaCO<sub>3</sub> is 10<sup>-4</sup> m<sup>3</sup> in standard temperature and pressure (STP) condition. This is half the volume of gas released by an equal amount of TiH<sub>2</sub>. This volume is higher than the expected release volume, as the matrix resists plastic deformation during gas release. The situation should eventually lead to lower porosity in the metal. However, the total volume of released gas disperses into a small volume due to the uniform and fine distribution of CaCO<sub>3</sub> particles between the thin aluminum layers, after ARB process (Fig. 4e). As mentioned, applying the ARB cycles leads to fracture of the blowing agent particles which distribute among different layers during ARB process, so the particles become finer than the initial size. This phenomenon, shown schematically in Fig. 5, explains how particles are fragmented during ARB cycles. Fig. 5 shows that when the particles are fractured and become smaller during ARB process, the free surface area of blowing agent increase. It is evident that efficiency of the chemical reaction goes up by increasing surface area and it leads to improve the kinetic of decomposition reaction.

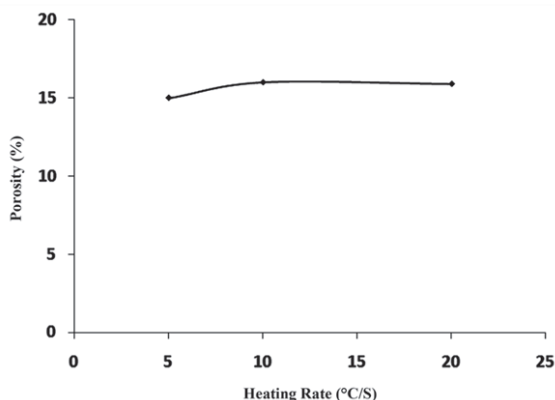


Fig. 6. Effect of heating rate on percent of porosity by foaming at 700°C for 3 min

Using small particles has both advantages and disadvantages. Fine particles decompose faster than the coarse particles, leading to time savings. However, very fine particles may be difficult to disperse in the melt, may agglomerate and release gas prematurely [17]. This drawback can be avoided during the ARB process when the fine blowing agent particles are inserted in the metallic matrix.

The effect of heating rate on foaming efficiency is shown in Fig. 6. Results show that the heating rate has no effect on percent of porosity during foaming process. Hence, the role of heating rate was ignored in further experiments and then samples were directly heated up from room to foaming temperature.

It has been shown [18] that decomposition of calcium carbonate powder starts at about 590 °C and ends around 840 °C. Thus, there is no significant difference between decomposition temperature of CaCO<sub>3</sub> and melting point of aluminum. Hence, during gas release at high temperatures, the aluminum matrix is soft enough to deform by the released gas and consequently, the blowing agent acts efficiently. The situation explains why foaming process is not affected by heating rate when calcium carbonate is employed

as the blowing agent. In other words, the strength of the aluminum matrix is reduced at this high temperature and it is consistent with decomposition of blowing agent. So, CaCO<sub>3</sub> starts to decompose thereby the gas expansion is accommodated as pores. It can also be concluded that preheating at 300 °C is not required for foaming by CaCO<sub>3</sub>.

A different situation exists in the foaming process with TiH<sub>2</sub>. The starting decomposition temperature of TiH<sub>2</sub> is not matched to the melting range of the aluminum [19]. Decomposition of TiH<sub>2</sub> starts around 400 °C [20] and the released gas cannot produce plastic deformation to form pores because of relatively high strength of the aluminum matrix at this temperature. So the sample should be heated abruptly to foaming temperatures in order to produce high porosity foam. Therefore, the effect of heating rate from decomposition temperature of TiH<sub>2</sub> to foaming temperature is relevant. Moreover, the difference between decomposition temperature of blowing agent and melting point of aluminum causes formation of irregular shape pores in early expansion stages, which could lead to irregularities in the final product [20]. For solving this problem, some work has been done to delay

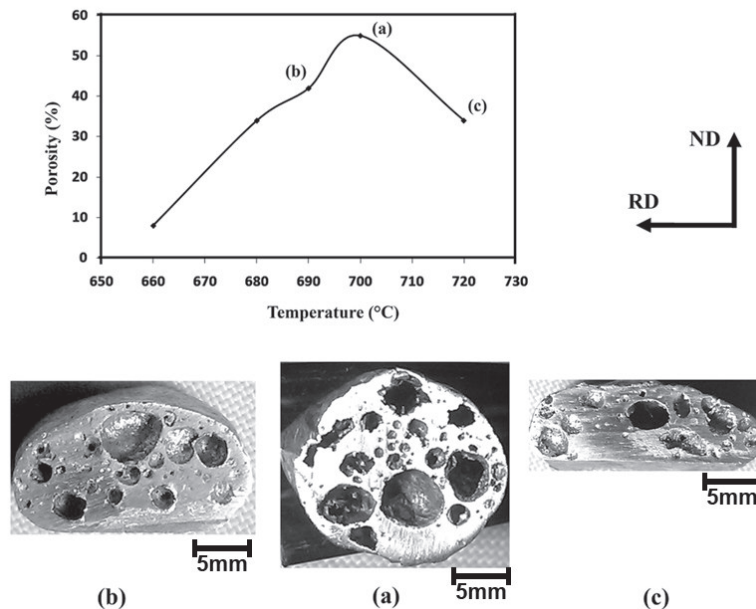


Fig. 7. Effect of foaming temperature on the percent of porosity at foaming time of 8 min

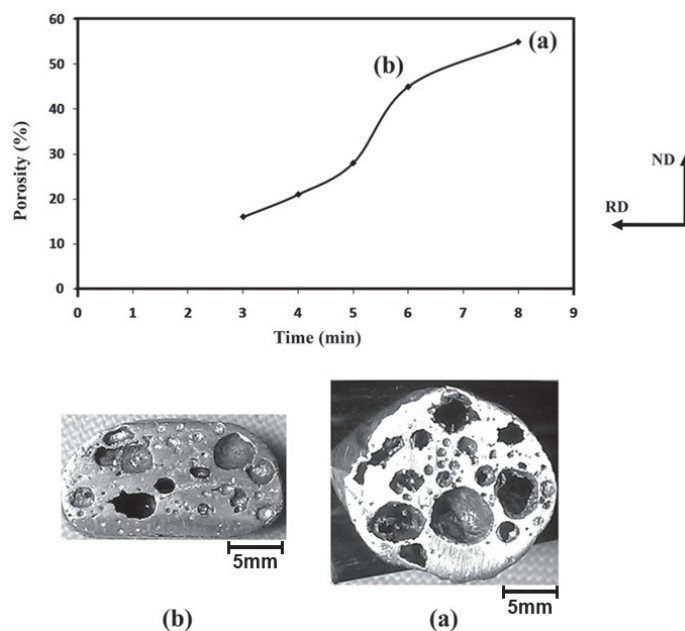


Fig. 8. Effect of holding time on the percent of porosity at foaming temperature of 700°C

the gas releasing initiation of  $\text{TiH}_2$  by surface treatments like oxidation,  $\text{Al}_2\text{O}_3$  or combined  $\text{Al}_2\text{O}_3/\text{SiO}_2$  coating of  $\text{TiH}_2$ [21].

The cell size of  $\text{CaCO}_3$  foamed material under optimum conditions is smaller than the hydride-foamed material despite the fact that the former foams were held at the foaming temperature for a longer time than that with  $\text{TiH}_2$  foaming agent[18]. Cell cracks were found only on hydride-foamed material[18]. For  $\text{CaCO}_3$ , the surface reaction of the released  $\text{CO}_2$  gas with aluminum leads to the formation of thin films of solid oxides and raises the mechanical stability of cells[22]. This phenomenon leads to increase the resistance from the cell walls against of cracks formation.

Fig. 7 shows the variation of porosity in the matrix with foaming temperature at a constant foaming time of 8 minutes. Maximum porosity was obtained at 700 °C, which is about 55%. Foaming temperature plays an important role on evolution of porosity. The efficiency of the chemical reactions is increased by increase temperature at constant holding time. This activates the reaction of blowing agent decomposition and amount of released gas is

increased. In this research, the optimum temperature and holding time for the foaming process were found to be 700 °C and 8 min, respectively. It is evident that beyond these optimum conditions, the porosity reduces because the matrix would be at the semi-solid state, so it can flow easily and the pore destroys and then gas escape from material[12]. As shown in Fig. 5e, the pores started to collapse at temperatures above 700 °C. Similar studies have shown 70% porosity using calcium carbonate as blowing agent of calcium carbonate by the PM route [18].

The graph shows that rate of porosity formation is low at temperature below 660 °C as the aluminum matrix has enough strength to resist pore formation. By increasing foaming temperature its strength reduces significantly and the rate becomes steep between 660 °C to 700 °C.

The effect of holding time on the percent of porosity is shown in Fig. 8. It shows that the porosity of the foam increases when the holding time of the samples at 700 °C is increased from 3 to 8 min. This may be attributed to the effect of holding time on the reaction kinetics of  $\text{CaCO}_3$  decomposition. This reaction cannot be completed

within short duration of foaming process. Therefore, the gas is less released and it causes less porosity. More decomposition takes place by increasing the holding time, which it results to release more gas and higher percentage of porosity.

#### 4. CONCLUSION

Aluminum closed-cell foam has been manufactured through the ARB process using calcium carbonate as the blowing agent. This blowing agent is an inexpensive material and results pleasant porosity and produces spherical pores and regular structure due to decent match of its decomposition temperature with melting point of the aluminum matrix. A different condition exists in the foaming process by  $TiH_2$ . In this case, the aluminum matrix is still strong enough when  $TiH_2$  starts to decompose and the released gas cannot produce plastic deformation to form pores. Therefore, the sample should be heated up abruptly to foaming temperatures in order to form more pores and increase percentage of porosity. In the present study, effect of heating rate, foaming temperature and holding time on pores formation was investigated and the following conclusions can be stated:

1. Increasing the number of ARB cycles leads to more fragmentation and uniform dispersion of blowing agent between aluminum layers.
2. Increasing the foaming temperature to 700 °C and holding time to 8 minutes results higher percentage of porosity, while increasing the foaming temperature beyond 700 °C leads to reduce the percentage of porosity.
3. Maximum porosity is obtained by up to 55% by use of calcium carbonate as foaming agent in optimum foaming condition.

#### REFERENCES

1. Sarajan, Z., Soltani, M., Kahani Khabushan, J., "Foaming of Al-Si by  $TiH_2$ ," *Materials and Manufacturing Processes*, 2011, 26, 1293-1298.
2. Sarajan, Z., Sedigh, M., "Influences of Titanium Hydride ( $TiH_2$ ) Content and Holding Temperature in Foamed Pure Aluminum",

- Materials and Manufacturing Processes, 2009, 24, 590-593.
3. Haijun, Y., Zhiqiang, G., Bing, L., Guangchun, Y., Hongjie, L., Yihan, L., "Research into the effect of cell diameter of aluminum foam on its compressive and energy absorption properties", *Materials Science and Engineering A*, 2007, 454-455, 542-546.
4. Arisetty, S., Ajay Prasad, K., Suresh, G., "Metal foams as flow field and gas diffusion layer in direct methanol fuel cells", *Journal of Power Sources*, 2007, 165, 49-57.
5. Shirzadi, A., Zhu, Y., Bhadeshia, H. K. D. H., "Joining Ceramics to Metals using Metallic Foam", *Materials Science and Engineering A*, 2008, 496, 501-506.
6. Schwingel, D., Seeliger, H. W., Vecchionacci, C., Alves, D., Dittrich, J., "Aluminium foam sandwich structures for space applications", *Acta Astronautica*, 2007, 61, 326-330.
7. Rostamzadeh, T., Shahverdi, H. R., "Microstructure study on Al-5% Si nanocomposite powders", *Iranian Journal of Materials Science & Eng.*, 2009, 8 (1), 32-39.
8. Kitazono, K., Kikuchi, Y., Sato, E., Kuribayashi, K., "Anisotropic compressive behavior of Al-Mg alloy foams manufactured through accumulative roll-bonding process", *Materials Letters*, 2007, 61, 1771-1774.
9. Moloodi, A., Raiszadeh, R., "Fabricating Al Foam from Turning Scraps", *Materials and Manufacturing Processes*, 2011, 26, 890-896.
10. Deng, W. J., Xia, W., Li, C., Tang, Y., "Ultrafine Grained Material Produced by Machining, *Materials and Manufacturing Processes*", 2010, 25, 355-359.
11. Tolaminejad, B., Karimi Taheri, A., Arabi, H., Shahmiri, M., "An investigation into the effect of ECAE process on mechanical and microstructural properties of middle layer in copper clad aluminum composite", *Iranian Journal of Materials Science & Eng.*, 2009, 6 (4).
12. Kitazono, K., Sato, E., Kuribayashi, K., "Novel manufacturing process of closed-cell aluminum foam by accumulative roll-bonding, *Scripta Materialia*", 2004, 50, 495-498.
13. Huang, X., Tsuji, N., Hansen, N., Minamino, Y., "Microstructural evolution during accumulative

- roll-bonding of commercial purity aluminum”, *Materials Science and Engineering A*, 2003, 340, 265–271.
14. Alizadeh, M., Paydar, M. H., “Study on the effect of presence of  $TiH_2$  particles on the roll bonding behavior of aluminum alloy strips”, *Materials and Design*, 2009, 30, 82–86.
15. Orłowicz, W., Tupaj, M., Mróz, M., Betlej, J., Płoszaj, F., “Effect of refining process on porosity and mechanical properties of high pressure Al-Si alloy die castings”, *Iranian Journal of Materials Science & Eng.*, 2012, 9 (1), 1–10.
16. Kurmaev, E. Z., Morozova, O., Khomenko, T. I., Borchers, C. H., Nemnonov, S. N., Harada, Y., Tokushima, T., Osawa, H., Takeuchi, T., Shin, S., “Local bonding structure in mechanically activated  $TiH_2$  and  $TiH_{2+}$  graphite mixture”, *Journal of Alloys and Compounds*, 2005, 395, 240–246.
17. Gergely, V., Curran, D. C., Clyne, T. W., “The FOAMCARP process: foaming of aluminium MMCs by the chalk-aluminium reaction in precursors”, *Composites Science and Technology*, 2003, 63, 2301–2310.
18. Cambroner, L. E. G., Ruiz-Roman, J. M., Corpas, F. A., Ruiz Prieto, J. M., “Manufacturing of Al–Mg–Si alloy foam using calcium carbonate as foaming agent”, *Journal of materials processing technology*, 2009, 209, 1803–1809.
19. Matijasevic, B., Banhart, J., “Improvement of aluminium foam technology by tailoring of blowing agent”, *Scripta Materialia*, 2006, 54, 503–508.
20. Matijasevic-Lux, B., Banhart, J., Fiechter, S., Gorke, O., Wanderka, N., “Modification of titanium hydride for improved aluminium foam manufacture”, *Acta Materialia*, 2006, 54, 1887–1900.
21. Fang, J., Ding, B., Yang, Z., Zhao, K., Gu, C., “The effect of  $SiO_2$  and  $Al_2O_3$  coating on the surface of  $TiH_2$  powders on gas release”, *Journal of Colloid and Interface Science*, 2005, 283, 1–4.
22. Papadopoulos, D. P., Omar, H., Stergioudi, F., Tsipas, S. A., Michailidis, N., “The use of dolomite as foaming agent and its effect on the microstructure of aluminium metal foams- Comparison to titanium hydride”, *Colloids Surf A*, 2011, 382, 118–123.